

Large Deflection of Prismatic Cantilever Beam Exposed to Combination of End Inclined Force and Tip Moment

Ibrahim Abu-Alshaikh¹, Hashem S. Alkhalidi¹ & Nabil Beithou²

¹ Mechanical Engineering Department, The University of Jordan, Jordan

² Mechanical Engineering Department, Tafila Technical University, Jordan

Correspondence: Ibrahim Abu-Alshaikh, Mechanical Engineering Department, The University of Jordan, Amman 11942, Jordan. E-mail: i.abualshaikh@ju.edu.jo, h.alkhalidi@ju.edu.jo, nabil.betthou@ttu.edu.jo

Received: September 9, 2017

Accepted: September 19, 2017

Online Published: December 28, 2017

doi:10.5539/mas.v12n1p98

URL: <https://doi.org/10.5539/mas.v12n1p98>

Abstract

The large deflection of a prismatic Euler-Bernoulli cantilever beam under a combination of end-concentrated coplanar inclined force and tip-concentrated moment is investigated. The angle of inclination of the applied force with respect to the horizontal axis remains unchanged during deformation. The cantilever beam is assumed to be naturally straight, slender, inextensible and elastic. The large deflection of the cantilever beam induces geometrical nonlinearity; hence, the nonlinear theory of bending and the exact expression of curvature are used. Based on an elliptic integral formulation, an accurate numerical solution is obtained in terms of an integration constant that should satisfy the boundary conditions associated with the cantilever beam. For some special cases this integration constant is exactly found, which leads to closed form solution. The numerical solution obtained is quite simple, accurate and involves less computational time compared with other techniques available in literature. The details of elastica and its corresponding orientation curves are presented and analyzed for extremely large load combinations. A comparative study with pre-obtained results has been made to verify the accuracy of the presented solution; an excellent agreement has been obtained.

Keywords: coplanar inclined force, Prismatic Cantilever Beam, large deflection, tip-concentrated moment

1. Introduction

Deflection of a cantilever beam (CB) has been the subject of numerous engineering problems nowadays which have very attractive civilian applications, e.g., shipbuilding, forestry, roofed structures, cranes, heavy bridges, flexible manipulator, etc. Thus, analyzing large deflections becomes a necessity while studying the kinematics and dynamics of flexible manipulators (Kimball et al., 2000). Large manipulator arms were originally developed for space research and used in many new applications concerning mechanical robot structures with relatively large spans. Compliant mechanisms are also composed of elastic links whose deformations are utilized to produce the desired output motion for a given input actuation. In comparison to a rigid body mechanism, a compliant mechanism yields smaller workspace (Banerjee et al., 2009; Tolou & Herder, 2009). Furthermore, large deformation of its links enforces the consideration of geometric and material non-linearity, thus making its design and synthesis a challenging task.

Many examples of a small deflection theory of a CB subjected to a vertical concentrated force at the free end can be found in many mechanics textbooks (Gere & Goodnoo, 2012). However, in the small deflection theory, the principle of superposition with small angle assumptions is valid and the equation of deflection shows proportionality between the deflection and the externally applied force. On the other hand, when deflections are large, the small angle assumption and the principle of superposition are no longer valid, the problem becomes increasingly difficult and the analytical solution for many loading conditions does not exist due to the presence of a nonlinear term in the governing equation. Elliptic integrals solution was also obtained for the large deflection of a CB subjected to one concentrated load, acting vertically downward at the free end of the beam (Braten, 1944; Bisshopp & Drucker, 1945). Based on the fundamental Euler-Bernoulli theorem, the large deflection of a CB under two concentrated loads in terms of elliptic integrals was solved in (Frisch-Fay, 1962). Analytical solution based on an elliptic integral formulation approach for analyzing the large deflection behavior of a guyed column pulled by a pre-tensioned cable for different deformed configurations was presented in (Yau, 2010).

In the middle of the 1980s, Adomian proposed a new and fruitful method, the so-called Adomian Decomposition Method (ADM), for solving linear and nonlinear ordinary, partial and integro-differential equations (Adomian, 1986). The ADM combined with the nonlinear shooting method have been proposed to determine the large deflection of a CB under arbitrary loading conditions (Banerjee et al., 2008). The nonlinear shooting method gave accurate numerical results while the ADM yields polynomial expressions for the beam configuration (Wazwaz, 2000). Geometrical nonlinear static analysis of an isotropic and hyper-elastic CB subjected to a non-follower transversal point end load was presented in (Kocatürk et. al, 2010), in which, the effects of large deflections and rotations on the displacements and normal and shear stress distributions through the thickness of the beam are investigated in detail. Deflection profiles of linear elastic tapered CB under arbitrary distributed loads were also obtained by means of a weighted residual solution of the Euler-Bernoulli bending moment equation (Baker, 1993). A linear elastic CB of variable cross-section under combined loading was investigated by means of the Runge-Kutta method (Lee et. al, 1993). The same method was used to investigate the large deflection of a CB of nonlinear elastic material under the effects of combined loadings (Lewis & Monasa, 1981; Lee, 2002). A uniform CB under the action of a combined load consisting of a uniformly distributed load and an external vertical concentrated load applied at the free end were analyzed (Belendez et. al, 2005; Belendez et. al, 2003; Belendez et. al, 2002). In these articles the numerical solution based on the Runge-Kutta-Fehlberg method was compared with experimental results. Expanding the slope in a power series of the arc length leads to an approximate solution for the large deflection of a CB subject to a uniformly distributed load (Rhode, 1953). A numerical method for calculating large deflections of a CB under uniform loading was presented (Seames & Conway, 1957). This numerical method assumed that the elastic axis of the beam could be approximated by a number of circular arcs tangent to one another at their points of intersection, using the Euler-Bernoulli equation to determine the radius of each circular arc.

Large deflection of a CB subjected to a follower force was examined by reducing a nonlinear two-point boundary-value problem to an initial-value problem by non-iterative change of variables technique (Shvartsman, 2007). The static analysis of the flexible non-uniform CB under a tip-concentrated and intermediate follower forces is considered (Shvartsman, 2009). A new technique for large deflection analysis of non-prismatic CB based on the integrated least square error of the nonlinear governing differential equation was presented (Dado & Al-Sadder, 2005). Large deflection problems of a uniform CB under a rotational distributed loading were formulated by means of a second order nonlinear integro-differential equation in (Rao B. & Rao G., 1989). The problem was numerically solved by considering a uniform rotational distributed load and a linearly varying rotational distributed load along the span of the beam.

Exact and numerical solutions of non-prismatic, nonlinear bi-modulus CB subjected to a tip moment by applying a power series approach to analytically solve highly nonlinear simultaneous first-order differential equations (Shatnawi & Al-Sadder, 2007; Baykara et. al, 2005). In these references, the stress-strain relationship of the nonlinear material was represented by the Ludwick constitutive law. However, these results showed that the bi-modulus behavior has a significant effect for the case of large deflection. The work presented in (Brojan et. al, 2007) analyzes large deflection profiles of slender, inextensible CB of prismatic and non-prismatic longitudinal shapes with rectangular cross-sections subjected to a concentrated end moment.

In this study, an accurate numerical solution for elastic prismatic CB subjected to a constant concentrated inclined load with a tip-moment is to be derived. During deformation, the angle of the inclined force remains unchanged with respect to the horizontal axis. In the presence of the tip-moment and the absence of the end load, this paper introduces a closed form expression for both the slope angle and deflection along the CB. Furthermore, a closed form solution is also obtained for the slope angle as the inclined load becomes infinity with the absence of the tip moment. However, for other case studies that have both inclined load with tip-concentrated moment the solution contains an arbitrary constant that can be found accurately by Newton Raphson method. On the other hand, Bisshopp and Drucker increase the value of the tip-angle consequently step by step until achieving the solution so that the absolute difference between the exact and approximate loading does not exceed the tolerance (Bisshopp & Drucker, 1945). In the absence of the tip moment, this incremental approach is applied only for orthogonal inclination loading angle where the elastica of the beam does exceed the vertical axis. Similar procedure applying Jacobi elliptic integrals of first and second types by considering only end-load is used by Howell and Midha (Howell & Midha, 1995). Saxena and Kramer proposed a numerical integration scheme that requires special consideration for the occurrence of any inflection point within the beam for combined end loading (Saxena & Kramer, 1998). Banerjee et al., used the ADM and non-linear shooting method by splitting the beam into several cantilevers each having only end loads. The ADM results are compared with the results presented by Bisshopp and Drucker for non-extremely large end loading conditions. However, the

ADM needs too many algebraic computations to achieve the required accuracy for more complicated loading conditions.

2. Problem Formulation

Consider an inextensible slender CB of length L with a constant flexural stiffness EI subjected to a concentrated non-follower end load P inclined with an angle δ measured from the positive x -axis and tip-moment $M(L)$. These loading conditions are presented in the global (x, y) coordinate-system, where the curved coordinate along the deflected axis of the beam is denoted by the arc length s , as shown in Fig. 1. The concentrated end force P is decomposed into two components F_x and F_y . Considering the free body diagram of the right segment of the beam, where the length of this segment becomes $(L-s)$, as shown in Fig. 2. Since the beam weight is assumed to be neglected, the horizontal and vertical static equilibrium equations lead that the components F_x and F_y are independent of the arc length s . However, the internal bending moment is a function of the arc length s , as shown in Fig. 3. In this figure, θ represents the angle of rotation of the beam with respect to the positive x -axis and ds denotes the length of infinitesimal element of the beam. Hence, the moment equilibrium equation of the beam can be written as

$$\frac{dM}{ds} = -F_x \frac{dy}{ds} - F_y \frac{dx}{ds} \tag{1}$$

where

$$\frac{dy}{ds} = \sin(\theta(s)), \quad \frac{dx}{ds} = \cos(\theta(s)) \tag{2}$$

$$M(s) = EI \frac{d\theta(s)}{ds} \tag{3}$$

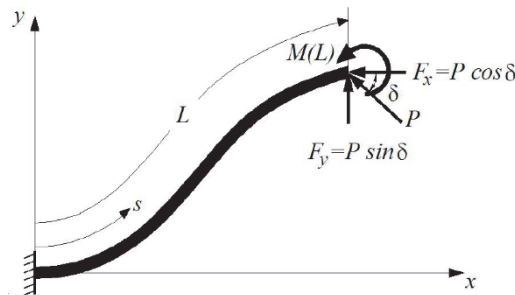


Figure 1. a CB subjected to concentrated end load and tip moment

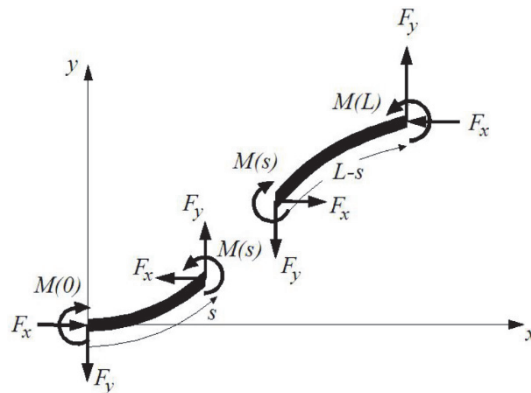


Figure 2. Free body diagram of the CB

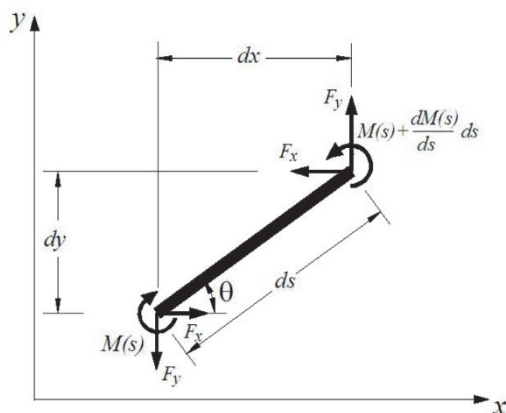


Figure 3. Infinitesimal element of the CB

Differentiating both sides of Eq. (3) with respect to the arc length s and substituting the resultant relation into Eq. (1) lead to

$$EI \frac{d^2\theta(s)}{ds^2} = -F_x \sin(\theta(s)) - F_y \cos(\theta(s)) \tag{4}$$

This differential equation governs the large deflection of the prismatic CB in terms of the slope of the beam $\theta(s)$ and the arc length s , as shown in Fig. 1. The components of the inclined load P can be written as

$$F_x = P \cos(\delta), F_y = P \sin(\delta) \tag{5}$$

Substituting Eq. (5) into Eq. (4) yields

$$\frac{d^2\theta(s)}{ds^2} = -\omega^2 \sin(\theta(s) + \delta) \tag{6}$$

where

$$\omega^2 = \frac{P}{EI} \tag{7}$$

The beam under consideration is associated with the following boundary conditions

$$\theta(0) = 0 \tag{8}$$

$$\left. \frac{d\theta(s)}{ds} \right|_{s=L} = \frac{M(L)}{EI} \tag{9}$$

Where $M(L)$ is the external moment applied at the free end of the beam. Although Eq. (6) is straightforward in appearance, it is in fact rather difficult to solve because of the nonlinearity term $\sin(\delta + \theta(s))$. In order to obtain the exact solution of Eq. (6), this equation is multiplied by $(d\theta(s)/ds)$, so that it becomes

$$\frac{d^2\theta(s)}{ds^2} \frac{d\theta(s)}{ds} + \omega^2 \sin(\theta(s) + \delta) \frac{d\theta(s)}{ds} = 0 \tag{10}$$

which can be rewritten as

$$\frac{d}{ds} \left[\frac{1}{2} \left(\frac{d\theta(s)}{ds} \right)^2 - \omega^2 \cos(\theta(s) + \delta) \right] = 0 \tag{11}$$

Equation (11), which corresponds to the conservation of mechanical energy, can be immediately rearranged by equating the term inside the square brackets by a constant C , as

$$\left(\frac{d\theta(s)}{ds}\right)^2 = [2C + 2\omega^2 \cos(\theta(s) + \delta)] \tag{12}$$

where C is an integrating constant that should satisfy one of the boundary conditions associated with the beam. Using the trigonometric relation

$$\frac{1 - \cos(\theta(s) + \delta)}{2} = \sin^2\left(\frac{\theta(s) + \delta}{2}\right) \tag{13}$$

Equation (12) can be reduced to

$$\frac{d\theta(s)}{ds} = 2\omega \sqrt{\frac{1}{\zeta^2} - \sin^2\left(\frac{\theta(s) + \delta}{2}\right)} \tag{14}$$

where

$$\zeta^2 = \frac{2\omega^2}{C + \omega^2} \tag{15}$$

To obtain the possible ranges of the end slope $\theta(L)$ corresponding to a particular load inclination angle δ , the expression for the curvature of the beam appears in Eq. (14) is examined. Noting that the sign of the term under the square root in Eq. (14) must be positive at all points on the beam including the free end; this is due to the fact that the curvature is always a real number. However, to ensure that this term is positive at the whole points of the beam, the following condition should be satisfied for every value of the arc length s along the beam

$$\frac{1}{\zeta^2} \geq \sin^2\left(\frac{\theta(s) + \delta}{2}\right) \tag{16}$$

Replacing the sine term in Eq. (14) by y_1 , where

$$y_1 = \sin\left(\frac{\theta(s) + \delta}{2}\right) \tag{17}$$

From Eq. (17), (dy_1 / ds) is obtained as a function of $(d\theta(s) / ds)$ by differentiating it with respect to s and squaring both sides

$$\left(\frac{dy_1}{ds}\right)^2 = \frac{1}{4}(1 - y_1^2) \left(\frac{d\theta(s)}{ds}\right)^2 \tag{18}$$

Substituting Eq. (14) into (18) gives

$$\frac{dy_1}{ds} = \sqrt{\frac{\omega^2}{\zeta^2} (1 - y_1^2)(1 - \zeta^2 y_1^2)} \tag{19}$$

Equation (19) is a separable first order ordinary differential equation which can be solved directly by integrating both sides as

$$\int ds = \frac{\zeta}{\omega} \int \frac{dy_1}{\sqrt{(1 - y_1^2)(1 - \zeta^2 y_1^2)}} \tag{20}$$

Perform the integration, Eq. (20) can be written in terms of elliptic integral as (Andrews, 1997)

$$F(y_1; \zeta) = \frac{\omega s}{\zeta} + C_1 \tag{21}$$

Applying the boundary condition presented in Eq. (8) leads to $C_1 = F(\sin(\delta / 2); \zeta)$. Equation (21) can be rewritten in terms of Jacobi elliptic function $sn[u; m]$ as (Andrews, 1997)

$$y_1 = sn\left[\frac{\omega s}{\zeta} + F(\sin(\delta / 2); \zeta); \zeta\right] \tag{22}$$

Using Eq. (17), the slope angle can be written as

$$\theta(s) = 2 \arcsin \left(sn \left[\frac{\omega s}{\zeta} + F(\sin(\delta/2); \zeta); \zeta \right] \right) - \delta \quad (23)$$

Introducing the following dimensionless parameters

$$\bar{s} = \frac{s}{L}, \bar{P} = \frac{PL^2}{EI}, \bar{\omega} = \omega L, \bar{M}(L) = \frac{LM(L)}{EI} \quad (24)$$

Eq. (23) can be presented in terms of the above non-dimensional quantities as

$$\theta(\bar{s}) = 2 \arcsin \left(sn \left[\frac{\bar{\omega} \bar{s}}{\zeta} + F(\sin(\delta/2); \zeta); \zeta \right] \right) - \delta \quad (25)$$

where δ and ζ are dimensionless quantities. Differentiating both sides of Eq. (27) with respect to \bar{s} will give (Andrews, 1997)

$$\frac{d\theta}{d\bar{s}} = \frac{2\bar{\omega}}{\zeta} dn \left[\frac{\bar{\omega} \bar{s}}{\zeta} + F(\sin(\delta/2); \zeta); \zeta \right] \quad (26)$$

where $dn[u; m]$ is the well-known type of Jacobi elliptic functions (Andrews, 1997). The quantity $\bar{\omega}$ represents the non-dimensional resultant force applied at the free end of the beam. From Eqs. (7), (24) $\bar{\omega}$ can be expressed as

$$\bar{\omega} = \sqrt{\bar{P}} \quad (27)$$

Equation (25) which satisfies automatically the boundary condition presented in Eq. (8), represents the exact solution of the problem. However, the integration constant ζ can be found directly from

$$M(1) = \frac{2\bar{\omega}}{\zeta} dn \left[\frac{\bar{\omega}}{\zeta} + F(\sin(\delta/2); \zeta); \zeta \right] \quad (28)$$

This equation is obtained from Eq. (26) applying the boundary condition at the free end presented in Eq. (9). As special case, when the beam is subjected to pure bending moment, i.e., $\bar{\omega} \rightarrow 0$ the value of ζ approaches zero, Eq. (15), and the integration constant C presented in Eq. (15) converges to $M^2(1)/2$. However, in this case the deflected shapes of the beam become circular arcs. The details of this special case will be illustrated in the next Section. Furthermore, in the absence of the tip-bending moment and as the load becomes very large ($\bar{\omega} \rightarrow \infty$), the value of ζ approaches plus unity when $\delta = \pi/2$, while when $\delta = -\pi/2$ the value of ζ approaches minus unity. Using the relation $\lim_{\zeta \rightarrow 1} sn(u; \zeta) = \tanh(u)$, Eq. (25) with ($\bar{\omega} \rightarrow \infty$ and $\zeta \rightarrow 1$) reduces to

$$\theta(\bar{s}) = 2 \arcsin \left(\tanh \left[\frac{\bar{\omega} \bar{s}}{\zeta} + F(\sin(\delta/2); \zeta) \right] \right) - \frac{\pi}{2} = \pi - \frac{\pi}{2} = \frac{\pi}{2} \quad (29)$$

In general, as $\bar{\omega} \rightarrow \infty$ then $\theta(\bar{s}) \rightarrow \pi - \delta$. This result indicates that the elastica of the beam will not exceed the difference $\pi - \delta$ which is due to the fact that the load is conservative. Thus, as the angle of the load inclination approaches zero, the CB will be deformed horizontally, i.e., parallel to the y-axis. In the above case studies as $\bar{\omega} \rightarrow 0$, this paper introduces a closed form expression for the slope angle and deflection along the CB. Moreover, as $\bar{\omega} \rightarrow \infty$ a closed form expression for the slope angle along the CB is obtained. Consequently, complicated iterative algorithms and methods are needed to find closed form solution for other load combinations. The proposed solution presented in Eq. (25) with the constant ζ which can be determined using Eq. (28) by Newton-Raphson method with a high accuracy. The proposed method solves the CB problem without: splitting the beam into several portions, applying any incremental or shooting methods and considering any inflection point conditions. A comparative study with pre-obtained results is performed to verify the solution even for extremely loading conditions which cannot be easily reached by other numerical techniques.

3. Results and Discussion

In this Section, all problems are analyzed in terms of the non-dimensional quantities prescribed in the previous section by ignoring the bar sign above the characters for simplification purposes. Two verification problems include combined load application at the free end of the beam will be analyzed and compared. Moreover, other

problems of pure vertical, horizontal and pure tip bending moment and combined loading will also be analyzed.

3.1 Verification Problems

In order to verify the results, two verification problems are considered. In the first problem, five different loading conditions applied to the free end of the CB are analyzed. The corresponding elastica shapes of these loading systems are drawn using the large deflection theory, as shown in Fig.4. These results are verified by comparing them with the large deflected shape of similar load combination obtained in (Dado & Al-Sadder, 2005). The formulation appeared in reference (Dado & Al-Sadder, 2005) was based on representing the angle of rotation of the beam by a polynomial on the position variable along the deflected beam axis. The coefficients of the polynomial are obtained by minimizing the integral of the residual error of the governing differential equation and by applying the beam boundary conditions (Dado & Al-Sadder, 2005). The comparison with reference (Dado & Al-Sadder, 2005) shows a very good agreement especially in the case of the lowest three curves. The comparison with the upper two curves is also acceptable but with a little deviation. The value of the integration constant ζ and the accuracy of solutions are shown in Table 1, however, from the data presented in Table 1, the upper two curves in Fig. 4 are precisely analyzed and therefore they are accurate. This accuracy appears in achieving the boundary conditions of Eq. (8) and (9) very precisely with error less than 10^{-35} .

The second verification problem has been compared with the work done by (Banerjee et al., 2009; Tolou & Herder, 2009). The non-linear shooting and Adomian decomposition methods were used to determine the large deflection of a CB under arbitrary loading conditions (Banerjee et al., 2009; Tolou & Herder, 2009). Comparing the results of this study with the corresponding similar case studies of loading conditions appear in reference (Banerjee et al., 2009; Tolou & Herder, 2009) shows a very good agreement in the elastic shapes of the deflected beam, magnitudes and orientations, as shown in Fig. 5. For example, the deflection of the tip end of the CB for the loading condition $F_x=0.1$, $F_y=0.2$ and $M(I)=0.6$ is computed as $x/L=0.24187869632$ and $y/L=0.95853701928$ which precisely satisfy the numerical results in reference (Banerjee et al., 2009; Tolou & Herder, 2009); given as $x/L=0.2418$ and $y/L=0.95847$.

3.2 Vertical Load Application

In this problem the beam is assumed to be subjected to a vertical load component $\delta = \pi / 2$ while the horizontal load component and the tip bending moment are assumed to be zero. If non-dimensional force P is directed downward, then $\delta = -\pi / 2$, on the other hand, if it is directed upward, then $\delta = \pi / 2$. Figures 6a and 6b show the deflection shapes and their orientations for the CB which is subjected to a vertical load component with $\delta = \pi / 2$. In these figures, the pair $(x/L, y/L)$ of the deflected curve of the beam is calculated numerically from Eq. (2) by Simpson's rule (4000 intervals).

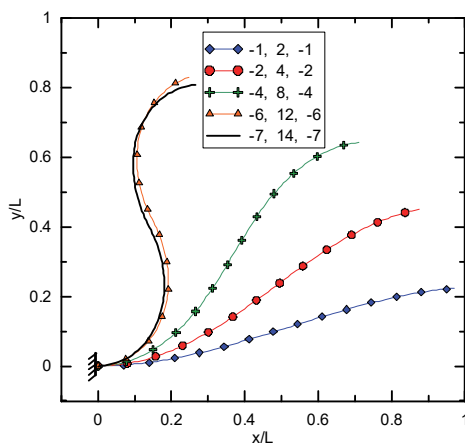


Figure 4. Elastica of a CB subjected to various dimensionless load combinations F_x , F_y and $M(I)$, respectively

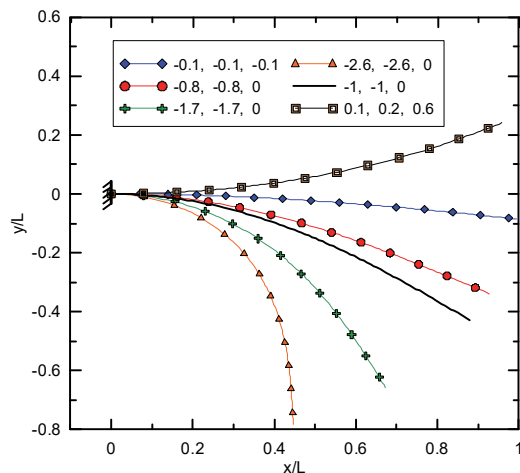


Figure 5. Elastica of a CB subjected to various dimensionless load combinations F_x , F_y and $M(l)$, respectively

It can be noted from the curves of Fig. 6a and Fig .6b that the deflection increases as the intensity of the load increases. Moreover, as the intensity of the load becomes very large the beam never crosses the y-axis, i.e., it runs parallel to it. For these curves, the solution is accurate for large non-dimensional load-intensity, the error in meeting the boundary conditions is very small, Table 1. From the curves in Fig. 6a and Fig .6b, one can also recognize that as the dimensionless load P increases from 1 to 4 the discrepancy in deflection is larger than that when the load P increases from 81 to 100; this is applicable when the non-linear elastic theory of beam deflection is applied. From Table 1, it can be clearly recognized how much the values of ζ for the non-dimensional load $P=100$ can satisfy the boundary conditions. Furthermore, we notice from Table 1 that as the intensity of the load becomes very large the value of ζ approaches plus unity, while when $\delta = -\pi / 2$ the value of ζ approaches minus unity. However, when $\zeta = \pm 1$ the solution presented in Eq. (25) becomes undefined in the absence of the horizontal load component and the tip bending moment. This is due to the fact that the force applied is a non-follower type and thus, the deflected beam never crosses the y-axis for this type of vertical loading.

3.3 Horizontal Load Application

In this problem the beam is assumed to be subjected to various non-dimensional force P with a small angle $\delta = \pi / 1000$, i.e., the vertical component of the applied force is assumed to be very small compared with the horizontal component, while the tip bending moment is assumed to be zero. If the vertical component vanishes, i.e., $\delta = 0$, the beam will not be bent anymore (stays horizontal), however this is true if the critical buckling-load is not exceeded. In here, if the axial compressive load exceeds the critical buckling-load the previous formulation should accordingly be changed. The small value of the vertical component is just an initiation for the beam to start deflecting upward. In other words, the overall resultant end load is almost horizontal and compressive. From Eq. (28), the values of ζ can be computed by Newton-Raphson technique for several intensity values of the applied non-dimensional load. In Table1 three values of the constant ζ are given for $P=64$, 81 and 100 with $\delta = \pi / 100$. Figures 7a and 7b show the deflection shapes for the CB for several loading conditions, from these curves it can be noted that the deflection increases as the intensity of the load increases. The obtained solution is also accurate for large load-intensity and the boundary conditions are satisfied to an extreme accuracy, Table 1.

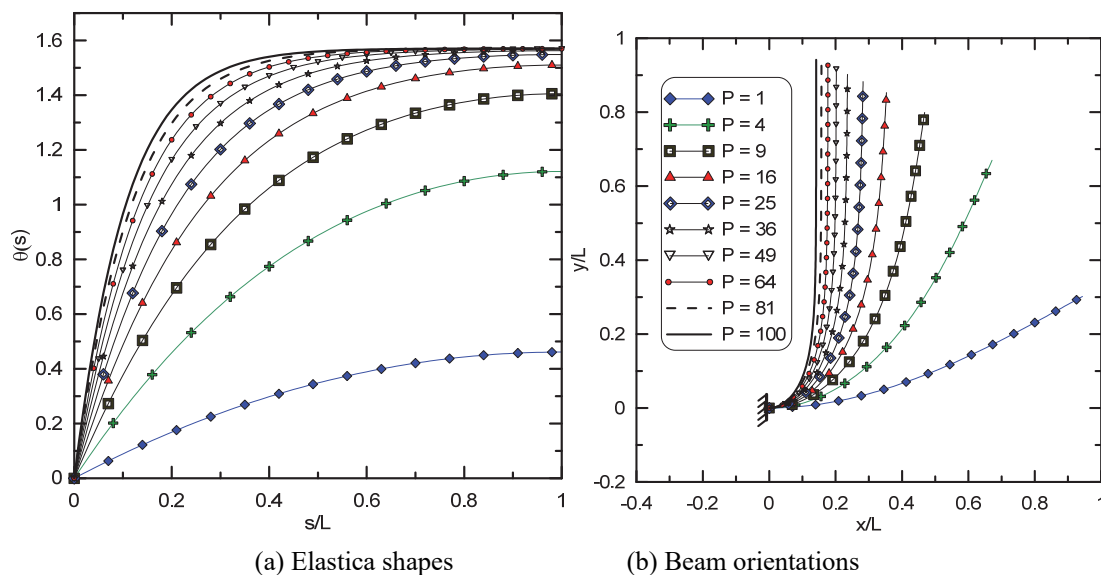


Figure 6. Elastica and orientations of a CB for various non-dimensional vertical loading conditions for $\delta = \pi / 2$, (common legend)

Table 1. Results obtained for several values of non-dimensional load application.

| Figure | \bar{P} | δ | $\bar{M}(1)$ | $\zeta, \theta(0), (d\theta/ds)(s=1), x/L, y/L$ |
|--------|--------------|----------------|--------------|---|
| Fig. 4 | $\sqrt{180}$ | $\tan^{-1}(2)$ | -6 | 0.951662353959048000707 0.0, -6.000000000000000 0.24717512667, 0.82837784901 |
| | $\sqrt{245}$ | $\tan^{-1}(2)$ | -7 | 0.957684836075187498093 0.0, -6.999999999999999 0.26664302022, 0.80707920248 |
| Fig. 6 | 64 | $\pi / 2$ | 0 | 1.0000001544640370108245 $1.00 \times 10^{-34}, 1.25 \times 10^{-30}$ 0.17677664068, 0.92677640568 |
| | 81 | $\pi / 2$ | 0 | 1.0000002090441485230536 0.0, 2.42×10^{-30} 0.15713483324, 0.93491257856 |
| | 100 | $\pi / 2$ | 0 | 1.00000002829104499453822 0.0, 1.40×10^{-30} 0.14142135393, 0.94142135086 |
| Fig. 7 | 64 | $\pi / 1000$ | 0 | 1.0000008974643621940573396 $-1.00 \times 10^{-37}, 2.71 \times 10^{-31}$ -0.74960191795 0.25235565250 |
| | 81 | $\pi / 1000$ | 0 | 1.0000001214578074080278522 $-1.00 \times 10^{-37}, 2.22 \times 10^{-31}$ -0.77742464456, 0.22466537703 |
| | 100 | $\pi / 1000$ | 0 | 1.0000000164375106401744599 $-1.00 \times 10^{-37}, 3.28 \times 10^{-30}$ |

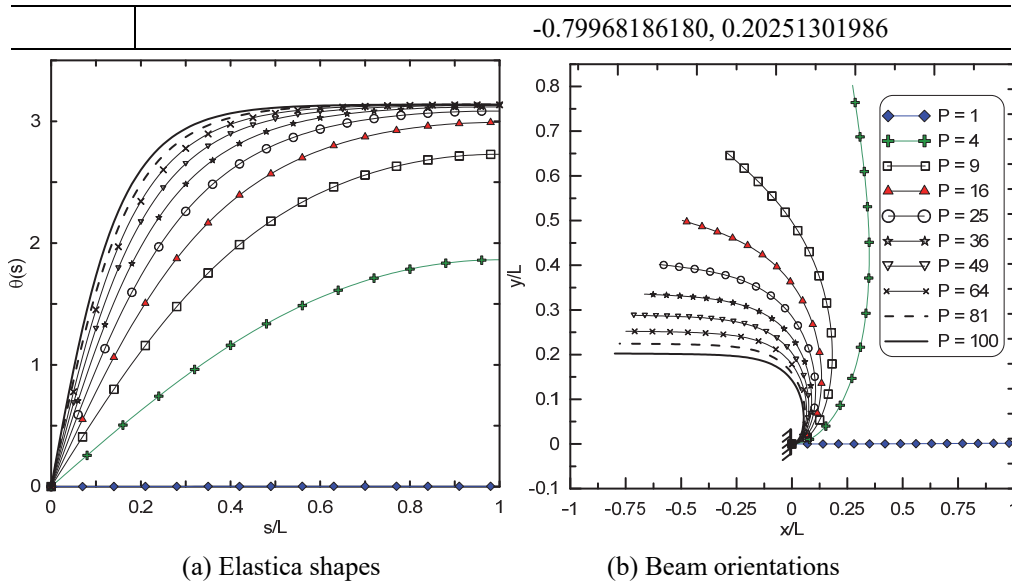


Figure 7. Deflection shapes and orientations of the CB for various dimensionless horizontal loading conditions for $\delta = \pi / 1000$, (common legend)

Furthermore, it can be recognized that the elastic curves will never cross the horizontal axis regardless the value of the intensity of non-dimensional applied load. Thus, when the load becomes extremely high with $\delta = \pi / 100$ the elastic curves will be closer to the horizontal axis due to the absence of the tip-moment $M(1)$. Similar trends of Fig.6 can also be recognized in Fig.7.

3.4 Pure Moment Application

In this section it is assumed that the CB is subjected to pure bending moment applied at the free end of the beam. Hence, in formulation it is assumed that the non-dimensional force P does not exist and therefore it approaches zero, i.e., $(\bar{\omega} \rightarrow 0)$. Furthermore, from Eq. (28) the value of ζ approaches to zero and the integration constant C presented in Eq. (15) converges to $(M^2(1)/2)$. Since both $\bar{\omega}$ and ζ approach to zero, and by applying L'Hopital's rule, the ratio $\bar{\omega} / \zeta$ approaches $(M(1)/2)$, i.e., by using Eq. (15)

$$\bar{\omega} / \zeta = \lim_{\bar{\omega} \rightarrow 0} \frac{\bar{\omega}}{\sqrt{2\bar{\omega}^2}} = \lim_{\bar{\omega} \rightarrow 0} \frac{\bar{\omega}}{\bar{\omega} \sqrt{\frac{2}{C + \bar{\omega}^2}}} = \sqrt{\frac{C}{2}} = M(1) / 2 \tag{30}$$

Substituting Eq. (30) into Eq. (25)

$$\theta(\bar{s}) = 2 \arcsin \left(\operatorname{sn} \left[\frac{M(1)\bar{s}}{2} + \frac{\delta}{2}; 0 \right] \right) - \delta \tag{31}$$

Hence, $\operatorname{sn}[\varphi; 0] = \sin(\varphi)$, (Andrews, 1997), Eq. (31) becomes

$$\theta(\bar{s}) = M(1)\bar{s} \tag{32}$$

In the above formulas $M(1)$ is the non-dimensional tip moment applied at the free end of the beam. Substituting Eq. (32) directly into Eq. (2) leads to the following relations

$$\frac{dx}{ds} = \cos(M(1)\bar{s}) \rightarrow x = \sin(M(1)\bar{s}) / M(1) + C_1 \tag{33}$$

$$\frac{dy}{ds} = \sin(M(1)\bar{s}) \rightarrow y = -\cos(M(1)\bar{s}) / M(1) + C_2 \tag{34}$$

The homogeneous boundary conditions at the fixed support, $x(0)=0$ and $y(0)=0$, lead that $C_1=0$ and $C_2=1/M(1)$. Equations (33) and (34) represent a circle of radius $1/M(1)$ centered at the point $(0, 1/M(1))$, which can be written as

$$x^2 + \left(y - \frac{1}{M(1)} \right)^2 = \left(\frac{1}{M(1)} \right)^2 \tag{35}$$

Equation (32) states that the slope of the elastica curves of the beam is simply related linearly to the non-dimensional arc length and it is deflected as a circle of radius $(1/M(1))$. However, the deflected shapes of the beam yield to: an arc of a circular shape when $(M(1) < 2\pi)$, a complete circle of a unity circumference when $(M(1) = 2\pi)$ or to an overlapped circular arcs when $(M(1) > 2\pi)$, as shown in Fig. 8 and Fig. 9. However, when $(M(1) > 0)$ the beam is deflected upward while when $(M(1) < 0)$ the beam is deflected downward. The closed form solution achieved through the Elliptic formulation stated above in Eq. (35) agrees with the recent results presented in (Tari, 2013 & Lin, 2010).

Referring to Eq. (27), the dimensionless tip moment $M(L)$ needed to bend any beam to a complete unit circle is $\bar{M}(L) = M(L)L / EI = 2\pi$. From this relation, it can be concluded that the deformed arc depends on $M(L)$, E , I and the length of the beam L . In other words, when $\bar{M}(L) = \pi$ the beam will be bent to a half circle of length unity, while when $M(L) = -4\pi$ the beam will rotate two times in two overlapped rings of length unity, as shown in Fig. 8 and Fig. 9. Hence, the actual moment needed to bend an elastic steel beam of $(E = 200 \text{ GPa}, L = 2.5 \text{ m})$ and a rectangular cross-sectional area of 1600 mm^2 to a semicircle is $M(L) = 53616.51464 \text{ N.m}$, while it requires double this amount to be bent to a complete circle.

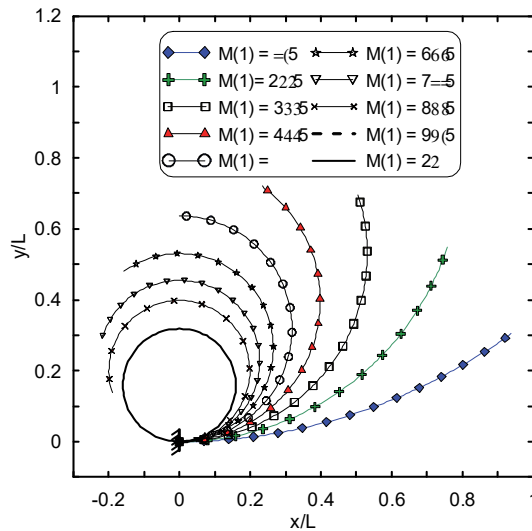


Figure 8. Deflection a CB subjected to various pure non-dimensional tip bending moments $M(1) < 2\pi$

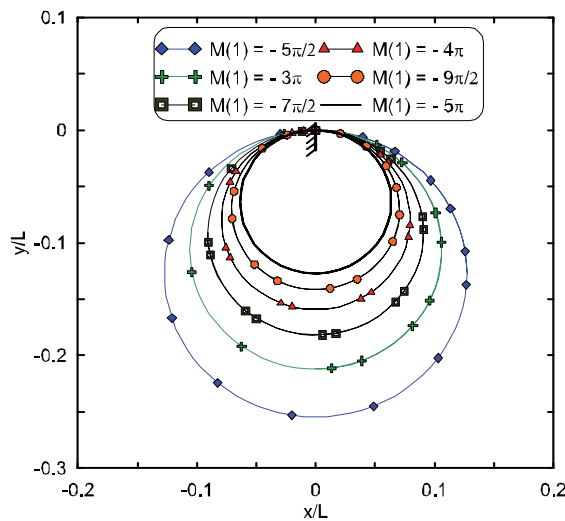


Figure 9. Deflection a CB subjected to various pure non-dimensional tip bending moments $M(1) > 2\pi$

3.5 Combined Loading Application

Deflection shapes and orientations of the CB subjected to non-dimensional force $P=4$ with $\delta = \pi / 4$ for various counterclockwise tip bending moments are presented in Fig.10. Increasing the moment will increase both the deflection and orientation of the beam and the deflected elastica curves tend to be bent to noncircular rings. These rings try to be closed with increasing the moment and they will stay open while the moment does not reach the value 2π , i.e., $M(1) < 2\pi$, as shown in Fig. 10a. When the tip moment exceeds the value of 2π , i.e., $M(1) > 2\pi$ with $P=4$ and $\delta = -\pi / 2$, the elastica curves will start to close and overcome the beam support but from inside the support, as shown in Fig. 11. On the other hand, the deflection shapes of the CB subjected to non-dimensional force $P=4$ with $\delta = \pi / 2$ for counterclockwise tip bending moments are presented in Fig.12. In this case, the elastica overcome the beam support from outside the support, as shown in Fig. 12.

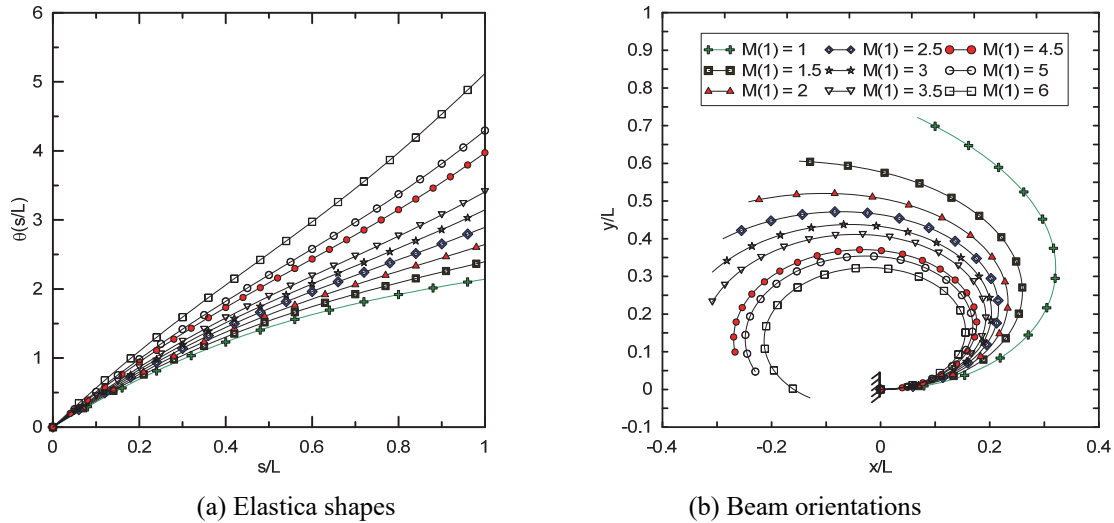


Figure 10. Elastica shapes and orientations of the CB subjected to dimensionless force $P=4$ with $\delta = \pi / 4$ and various tip bending moments, (common legend)

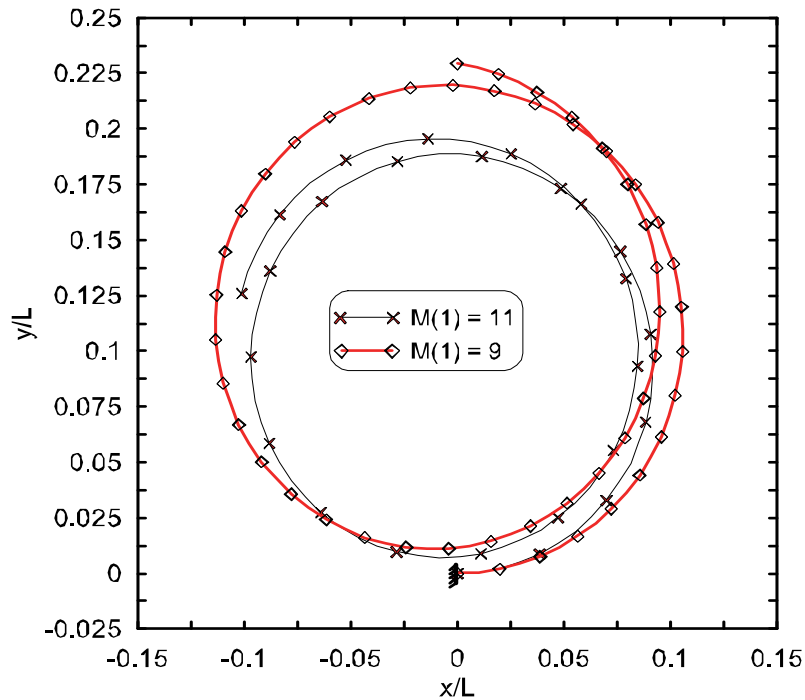


Figure 11. Helical rings of the CB subjected to dimensionless $P=4$ with $\delta = -\pi / 4$

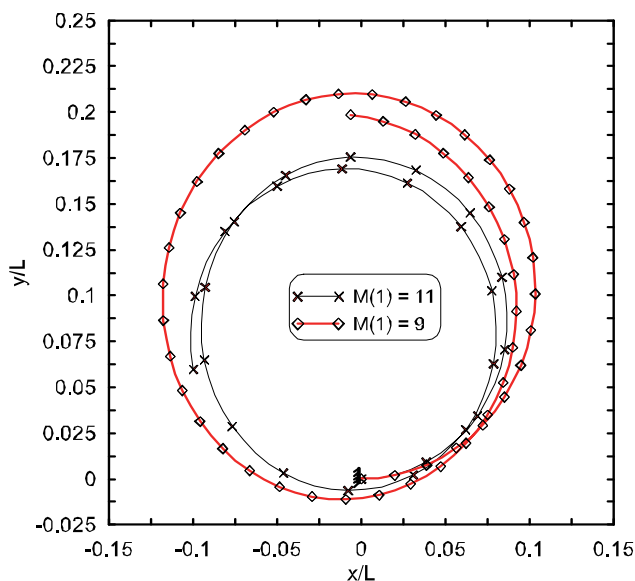


Figure 12. Helical rings of the CB subjected to a non-dimensional $P=4$ with $\delta = \pi / 4$

4. Conclusions

In this study, an accurate solution by means of elliptic integrals for deflections and orientations of a prismatic CB with large deflection are obtained. The beam is assumed to be subjected to a concentrated coplanar inclined force and tip-concentrated moment at its free end. The closed-form solution for deflection is further obtained for deflections and orientations when the CB is subjected to pure bending moment, for some other cases, a very accurate numerical solution is also obtained in terms of integration constant that satisfy the boundary conditions associated with the beam. However, to interpret the elastica curves of the CB, this integration constant is extracted numerically with low effort and high accuracy. Finally, the method applied in this study may be applied further to other non-linear beam problems with various types of follower, non-follower, concentrated or distributed loading with various boundary conditions to obtain possible analytical solutions.

References

- Adomian, G. (1986). *Nonlinear Stochastic Operator Equations*. Academic Press, San. Diego.
- Andrews, L. (1997). *Special Functions of Mathematics for Engineers*. SPIE Publications, Ohio.
- Baker, G. (1993). On the large deflections of non-prismatic cantilevers with a finite depth. *Computers and Structures*, 46, 365-370.
- Banerjee, A., Bhattacharya, B., & Mallik, A. K. (2008). Large deflection of CBs with geometric non-linearity: Analytical and numerical approaches. *International Journal of Non-Linear Mechanics*, 43, 366-376.
- Banerjee, A., Bhattacharya, B., & Mallik, A. K. (2009). Forward and inverse analyses of smart compliant mechanisms for path generation. *Mechanism and Machine Theory*, 44, 369-381.
- Barten, H. J. (1944). On the deflection of a CB. *Quarterly of Applied Mathematics*, 2, 168-171.
- Baykara, C., Guven, U., & Bayer, I. (2005). Large deflections of a CB of nonlinear bimodulus material subjected to an end moment. *Journal Reinforced Plastics Composites*, 24, 1321-1326.
- Belendez, T., Neipp, C., & Belendez, A. (2002). Large and small deflections of a CB. *European Journal Physics*, 23, 371-379.
- Belendez, T., Neipp, C., & Belendez, A. (2003). Numerical and experimental analysis of a CB: A laboratory project to introduce geometric nonlinearity in mechanics of materials. *International Journal Engineering Education*, 19, 885-889.
- Belendez, T., Perez-Polo, M., Neipp, C., & Belendez, A. (2005). Numerical and experimental analysis of large deflections of CBs under a combined load. *Physica Scripta*, 118, 61-65.
- Bisshopp, K. E., & Drucker, D. C. (1945). Large deflections of CBs. *Quarterly of Applied Mathematics*, 3, 272-275.

- Brojan, M., Videnic, T., & Kosel, F. (2007). Non-prismatic non-linearly elastic CBs subjected to an end moment. *Journal Reinforced Plastics Composites*, 26, 1071-1082.
- Dado, M., & AL-Sadder, S. (2005). A new technique for large deflection analysis of non-prismatic CBs. *Mechanics Research Communications*, 32, 692-703.
- Frisch-Fay, R. (1962). Large deflections of a CB under two concentrated loads. *Journal of Applied Mechanics*, 29, 200-201.
- Gere, J. M., & Goodnoo, B. (2012). *Mechanics of Materials*, (8th Ed.), Cengage Learning, Canada, 755-761.
- Howell, L. L., & Midha, A. (1995). Parametric deflection approximations for end-loaded large deflection beams in compliant mechanisms. *ASME Journal Mechanical Design*, 117, 156-165.
- Kimball, C., Tsai, L. W., DeVoe, D. L., & Maloney, J. (2000, July). Modeling and batch fabrication of spatial micro-manipulators. *Proceeding ASME Design Engineering Technical Conference*, Baltimore, MD.
- Kocatürk, T., Akbaş, Ş. D., & Şimşek, M. (2010). Large deflection static analysis of a CB subjected to a point load. *International Journal Engineering and Applied Sciences*, 2, 1-13.
- Lee, B. K., Wilson, J. F., & Oh, S. J. (1993). Elastica of cantilevered beams with variable cross sections. *International Journal of Non-Linear Mechanics*, 28, 579-589.
- Lee, K. (2002). Large deflections of CBs of non-linear elastic material under a combined loading. *International Journal of Non-Linear Mechanics*, 37, 439-443.
- Lewis, G., & Monasa, F. (1981). Large deflections of CBs of non-linear materials. *Computers and Structures*, 14, 357-360.
- Lin, C. W. (2010). Finite deformation of 2-D thin circular curved laminated beams. *Hsiuping Journal*, 22, 19-34.
- Rao, B. N., & Rao, G. V. (1989). Large deflections of a CB subjected to a rotational distributed loading. *Forschung im Ingenieurwesen*, 55, 116-120.
- Rhode, F. V. (1953). Large deflections of CBs with uniformly distributed load. *Quarterly of Applied Mathematics*, 11, 337-338.
- Saxena, A., & Kramer, S. N. (1998). A simple and accurate method for determining large deflections in compliant mechanisms subjected to end forces and moments. *ASME Journal Mechanical Design*, 120, 392-400.
- Seames, A. E., & Conway, H. D. (1957). A numerical procedure for calculating the large deflections of straight and curved beams. *Journal of Applied Mechanics*, 24, 289-294.
- Shatnawi, S., & AL-Sadder, S. (2007). Exact large deflection analysis of non-prismatic CBs of nonlinear bimodulus material subjected to a tip moment. *Journal Reinforced Plastics Composites*, 26, 1253-1268.
- Shvartsman, B. S. (2007). Large deflections of a CB subjected to a follower force. *Journal of Sound and Vibration*, 304, 969-973.
- Shvartsman, B. S. (2009). Direct method for analysis of flexible CB subjected to two follower forces. *International Journal of Non-Linear Mechanics*, 44, 249-252.
- Tari, H. (2013). On the parametric large deflection study of Euler-Bernoulli CBs subjected to combined tip point loading. *International Journal of Non-Linear Mechanics*, 49, 90-99.
- Tolou, N., & Herder, J. L. (2009). A semi analytical approach to large deflections in compliant beams under point load. *Journal of Mathematical Problems in Engineering*, 910896. <https://doi.org/10.1155/2009/910896>
- Wazwaz, A. (2000). A new algorithm for calculating Adomian polynomials for nonlinear operators. *Applied Mathematics Computations*, 111, 53-69.
- Yau, J. D. (2010). Closed-form solutions of large deflection for a guyed cantilever column pulled by an inclination cable. *Journal of Marine Science and Technology*, 18, 130-136.

Copyrights

Copyright for this article is retained by the author(s), with first publication rights granted to the journal.

This is an open-access article distributed under the terms and conditions of the Creative Commons Attribution license (<http://creativecommons.org/licenses/by/4.0/>).